in vivo *36*: 657-666 (2022)
doi:10.21873/invivo.12750

In Vivo Imaging of Ischemia/Reperfusion-mediated Aminopeptidase N Expression in Surgical Rat Model Using ^{68}Ga-NOTA-c(NGR)

GERGELY FARKASINSZKY[1,2], NOÉMI DÉNES[1,2], SZILVIA RÁCZ[3], ADRIENN KIS[1,4], JUDIT SZABÓ PÉLINÉ[1,4], GÁBOR OPPOSITS[1], GERGŐ VERES[3], LÁSZLÓ BALKAY[1], ISTVÁN KERTÉSZ[1], GÁBOR MEZŐ[5,6], JÁNOS HUNYADI[7#] and GYÖRGY TRENCSÉNYI[1,2,4#]

[1]Division of Nuclear Medicine and Translational Imaging, Department of Medical Imaging, Faculty of Medicine, University of Debrecen, Debrecen, Hungary;
[2]Gyula Petrányi Doctoral School of Allergy and Clinical Immunology, Faculty of Medicine, University of Debrecen, Debrecen, Hungary;
[3]Division of Radiology, Department of Medical Imaging, Faculty of Medicine, University of Debrecen, Debrecen, Hungary;
[4]Doctoral School of Clinical Medicine, Faculty of Medicine, University of Debrecen, Debrecen, Hungary;
[5]Eötvös Loránd University, Faculty of Science, Institute of Chemistry, Budapest, Hungary;
[6]MTA-ELTE, Research Group of Peptide Chemistry, Hungarian Academy of Sciences, Eötvös L. University, Budapest, Hungary;
[7]Department of Dermatology, University of Debrecen, Debrecen, Hungary

Abstract. *Background/Aim: Previous studies have already shown that ^{68}Gallium(^{68}Ga)-labeled NGR-based radiopharmaceuticals specifically bind to the neoangiogenic molecule Aminopeptidase N (APN/CD13). The aim of this study was to evaluate the applicability of ^{68}Ga-NOTA-c(NGR) in the in vivo detection of the temporal changes of APN/CD13 expression in the diabetic retinopathy rat model using positron emission tomography (PET). Materials and Methods: Ischemia/reperfusion injury was initiated by surgical ligation of the left bulbus oculi of rats. In vivo PET imaging studies were performed after the surgery using ^{68}Ga-NOTA-c(NGR). Results: Significantly higher ^{68}Ga-NOTA-c(NGR) uptake was observed in the surgically-ligated left bulbus, compared to the bulbus of the non-surgical group at each investigated time point. The western blot and histological analysis confirmed the increased expression of the neo-angiogenic marker APN/CD13. Conclusion: ^{68}Ga-NOTA-c(NGR) is a suitable radiotracer for the detection of the temporal changes of the ischemia/reperfusion-mediated expression of APN/CD13 in the surgically induced diabetic retinopathy rat model.*

[#]These Authors contributed equally to this study.

Correspondence to: György Trencsényi, Division of Nuclear Medicine and Translational Imaging, Department of Medical Imaging, Faculty of Medicine, University of Debrecen, 4032, Debrecen, Nagyerdei krt. 98. Debrecen, Hungary. Tel: +36 52255000/56194, Fax: +36 52 255500/56436, e-mail: trencsenyi.gyorgy@med.unideb.hu

Key Words: Aminopeptidase N, Angiogenesis, 68Ga-NOTA-c(NGR), ischemia/reperfusion, NGR peptide, positron emission tomography.

Diabetes mellitus (DM) belongs to the cluster of metabolic disorders, characterized by hyperglycemia over a prolonged interlude. Symptoms of hyperglycemia include polyuria, polydipsia, and polyphagia (1, 2). DM may cause many acute or severe complications (3), such as cardiovascular disease, stroke, chronic kidney failure, neuropathy and diabetic retinopathy (DR) (2, 4). DR is one of the most common microvascular complications of diabetes. In 2015, there were more than 414 million people affected by some form of diabetes. According to certain predictions, the number of diabetic patients will have extended to 641 million in 2040 (5). Diabetes can generally be divided into three types: i) insulin-dependent, ii) insulin-independent and iii) gestational, although, all patients commonly experience hyperglycemia. According to the current scientific evidence, approximately 33% of diabetic patients have signs of DR and approximately 10% of them even develop vision-threatening retinopathy (6). Clinically, DR-induced

retinopathy is classified as nonproliferative (NPDR) and proliferative (PDR) (7). From this aspect, the number of patients who potentially suffer from severe vision loss as a consequence of proliferative DR is more than ten million worldwide (8). Neovascularization of the retina leading to formation of new blood vessels, can be caused by PDR. The same process can be observed normally during wound healing and embryogenesis, but is also present in several human pathological disorders, such as tumours. Related to tumor- associated new blood vessel formation, Aminopeptidase N [APN/CD13 (Cluster of Differentiation: 13)] is a target of extensive research (9-11). Previous studies have revealed that APN/CD13 is selectively recognized by peptides containing the Asn-Gly-Arg (NGR) sequence. This tumour-homing motif was discovered by phage display technologies (12), with its circularization resulting in a ten-fold increase in the tumor target as this minimized its entropic cost of binding to the tumor (13). The applied cyclic analogue of NGR (c[KNGRE]-NH2) sequence is known as a possible biomarker of neovascularization (14, 15). ^{68}Gallium (^{68}Ga)-labeled cyclic NGR peptides could be a useful tool for preclinical positron emission tomography (PET), functioning as a noninvasive nuclear medicine-related imaging technique, which can be used to examine various pathophysiological processes (16-19). Specifically, PET imaging may be able to identify molecular modifications in an organ or tissue, thus, detect the initiation of a diabetic disease before structural changes are otherwise visible (20, 21).

The aim of this study was to evaluate the applicability of ^{68}Ga-NOTA-c(NGR) in the *in vivo* detection of the ischemia/reperfusion (IR)-mediated temporal changes of APN/CD13 expression in the diabetic retinopathy rat model using preclinical PET.

Materials and Methods

Radiopharmaceuticals. The APN/CD13-specific ^{68}Ga-NOTA-c(NGR) and the $\alpha_V\beta_3$ integrin-specific ^{68}Ga-1,4,7-triazacyclononane,1-glutaric acid-4,7-acetic acid (NODAGA)-[c(RGD)]$_2$ radiopharmaceuticals were synthesized according to the description of Máté *et al*. (2015) (14) at the University of Debrecen, Hungary, at the Department of Medical Imaging. The carrier vector, NGR peptide, conjugated with the NOTA chelator was prepared successfully, the in all isolated yield of the precursor after preparative HPLC was 47%. The conjugation of the chelator resulted in no significant loss of its original affinity and selectivity. ^{68}Ga-NOTA-c(NGR) was produced with high specific activity (5.17-5.93 GBq/μmol) and excellent radiochemical purity (>95%) for all the experiments it was used in.

Experimental animals. Male Fischer-344 rats (n=15; Animalab Ltd, Budapest, Hungary) aged 16 weeks and weighing 250-300 g were used in the experiments. Humane care was provided for all the animals in compliance with the Association for Research in Vision and Ophthalmology (ARVO) Statement for the Use of Animals in Ophthalmic and Vision Research and National Institutes of Health (NIH) guidelines (22). The conditions for accommodation, husbandry, and maintenance of the animals were met with the current regulations (23±2˚C with 50±10% humidity). This animal model is suitable for efficacy testing and surgical intervention-related purposes (23-25). The protocols were performed by certificated personnel (Federation of Laboratory Animal Science Associations). The rodents were randomly assigned to the certain groups. Experimental animals were held in individually ventilated cage system (IVC) racks (no of animals/cage=2). Nesting material and hiding place were provided as environmental enrichment. The rats were supplied with regular rodent food ["VRF-1" (Special Diets Services (SDS) Diets)] and water *ad libitum*. Light-dark cycle (12:12 h) was maintained. The animals were anaesthetized using an isoflurane anaesthesia chamber: Isoflurane 3% (AbbVie OGYI-T-1414/01), oxygen 0.4 l/min (Linde OGYI-T-20607), nitrous oxide 1.2 l/min (Linde OGYI-T-21090) in order to start and maintain analgesia during all experimental procedures. Their body temperature was kept within normal range (37.0-37.5˚C), continuously monitored by a temperature control system. Following successful anaesthesia, euthanasia of the experimental animals was performed using the isoflurane Anaesthesia chamber, with a cocktail of isoflurane 5% and nitrous oxide 1.2 l/min.

All of the protocols used in the present study were approved by the Institutional Animal Care Committee of the University of Debrecen, Hungary (approval number: 21/2017/DEMÁB).

Surgically induced-DR in rat model. Following anaesthesia, unilateral ligation of the nervus opticus, arteria ophthalmica and arteria ciliares was performed in accordance with the established protocol (26). The left eye of the rats (n=10) was ligated surgically, using a cannula guided loop. Ischemia was induced by tightening the noose for 90 min and then reperfusion by loosening it. The aforementioned surgical procedure is considered suitable for developing lesions that can occur during reperfusion (27, 28). Following the procedure, antibiotic eye drops were used to avoid possible inflammatory processes. As each eye's location is found symmetrically inside the skull, interpretating the results from these experiments offers the added benefit of the contralateral eye serving as an internal control, in addition to comparing it to other experimental groups (29).

Non-surgical control group. The use of sham-operated controls would mean pulling out the contralateral eye from the I/R-operated one. As this process would likely cause tissue and vascular injury and subsequently would healing, the expression of angiogenic factors would be different from normal basal levels (30, 31), causing a differential uptake of radiopharmaceuticals and increase of the SUV values. So the we avoid complicating the evaluation of our PET data, instead of using sham-operated animals, our control animals (n=5) were left untreated, kept under the same animal housing conditions and anesthetized/euthanazed using the same protocol as the one used for the animals in the surgically-induced group. The animals were maintained according to the standard study protocol.

Small animal PET imaging using ^{68}Ga-NOTA-c(NGR). On days 1, 3, 7 and 10 following ocular I/R surgically ligated and control rats were anaesthetized and injected with ^{68}Ga-NOTA-c(NGR) or ^{68}Ga-NODAGA-[c(RGD)]$_2$ (approximately 15 MBq in 150 μl saline) *via*

the lateral tail vein. Physiological body temperature of the anaesthetized experimental animals was maintained with the use of a heated camera bed. The distribution of the radiopharmaceuticals was determined 90 min post injection by *in vivo* PET imaging (MiniPET-II small animal PET scanner, University of Debrecen, Hungary) (20-min static PET scans) (32). Following the last PET investigation, animals were euthanized, and the eyes were subjected to further *ex vivo* measurements after proper preparation.

PET data analysis. The radiotracer uptake was expressed in terms of standardized uptake values (SUV). The region of interest (ROI) was determined manually around the eyes. The findings were visually assessed by the BrainCad software. SUV mean values were calculated using PET scanner analysis software tools, as follows: SUV=[ROI activity (Bq/ml)]/[injected activity (Bq)/animal weight (g)], assuming a density of 1 g/ml. A signal-to-background ratio (SBR) value was introduced for further statistical analysis. SBR value was determined individually for each experimental animal (SBR=SUVmean of left bulb/SUVmean of right bulb).

Western blot analysis. Ten days after the appropriate bulbus enucleation procedure, samples were suspended in lysis buffer of 20 mM Tris-HCl, pH 7.4, 5 mM EGTA, 1 mM 4-(2-aminoethyl)benzenesulfonyl fluoride (AEBSF, Thermo Fisher Scientific Inc., Waltham, MA, USA), protease inhibitor cocktail (1:100 dilution). At the same time, frozen bulbi immersed in liquid nitrogen were homogenized using a specific pestle and mortar. Subsequently, the obtained homogenate was dissolved in lysis buffer. An adapted BCA protein assay (Pierce™ BCA Protein Assay Kit, Thermo Fisher Scientific Inc.) was used to determine the protein content of the samples. The samples were then applied to electrophoresis in 10% sodium dodecyl sulfate-polyacrylamide gel [loaded with equal amount of protein per lane (20-60 μg)], transferred to nitrocellulose membranes (BioBond -Whatman, GE Healthcare Bio-Sciences AB, Uppsala, Sweden), and then probed with monoclonal mouse-anti-rat APN/CD13 and mouse-anti-rat integrin alphaV/beta3 [both from Santa Cruz Biotechnology Inc. Dallas, TX, USA); 1:100 dilution PBS (5% milk)]. Horseradish peroxidase-conjugated mouse IgG Fc segment-specific antibodies (source: goat, 1:1,000) Bio-Rad (Hercules, CA, USA) were used as secondary antibodies, and immunoreactive bands were imaged using the SuperSignal® West Pico® Chemiluminescent Substrate enhanced chemiluminescence kit (Thermo Fisher Scientific Inc.) and a KODAK Gel Logic 1500 Imaging System (Eastman Kodak Company, Rochester, NY, USA). In order to determine equal loading, the membranes were re-probed with anti-β-actin antibodies (1:1,000 dilution PBS in 5% milk) and visualized as mentioned above (14). ImageJ (Scion Corporation) was used for the quantification of band density. Sub results were collected automatically using densitometric measurements expressed in arbitrary units (AU) (33).

Histopathological analysis. Retinal neovascularization was examined by histopathological examination according to the established protocol (34). Bulbi were enucleated and embedded in cryomatrix (Thermo Fisher Scientific). Samples were cut in 9μm thick sections using cryotome (Thermo Fisher Scientific), and fixed in 10% buffered neutral formalin for 5 min. After washing out the redundant formalin, the selected sections were stained using hematoxylin-eosin.

Statistical analysis. Data shown on the charts are the results of at least three independent series of measurements presented as mean±SD. Student's two-tailed *t*-test, two-way ANOVA and the Mann-Whitney rank-sum tests were used for determining significance under null hypothesis. The significance level was set at $p<0.05$. A commercial software package (MedCalc 18.5, MedCalc Software, Mariakerke, Belgium) was used for all statistical analyses.

Results

In vivo longitudinal study of APN/CD13 expression in surgically induced rat model with ^{68}Ga NOTA-c(NGR). For the evaluation of the temporal changes in the expression of APN/CD13 in the surgically-induced rat model *in vivo* PET imaging was used. In this longitudinal study, the APN/CD13 specific ^{68}Ga-NOTA-c(NGR) accumulation of the ligated bulbs was compared to the healthy control eyes of the control group, and to the non-ligated eyes in the opposite bulb of the surgical group, as an internal control.

The qualitative analysis of the PET images showed no ^{68}Ga-NOTA-c(NGR) accumulation in either eye of the rats in the non-surgical control group. In contrast, remarkable radiotracer accumulation was found in the surgically ligated bulbs from 3 days after the surgery. Interestingly, remarkable radiotracer uptake was also observed in the non-ligated opposite bulbs of the surgical group ten days after the surgery (Figure 1A). After the quantitative analysis of the decay-corrected PET images, significantly ($p\leq0.01$) increased ^{68}Ga-NOTA-c(NGR) uptake was observed in the surgically ligated eyes of the surgical group, where the SUVmean values were 0.35±0.06, 0.29±0.05 and 0.33±0.04 3, 7 and 10 days after the surgery, respectively (Figure 1B). At the first investigated time point (1 day after the surgery) there was no significant difference (at $p\leq0.05$) between the SUVmean values of the ligated (I/R) and non-ligated eyes (non-I/R). Figure 1B demonstrates that 3 and 7 days after the surgery the ^{68}Ga-NOTA-c(NGR) uptake of the ligated eyes was approximately two-times higher compared to that of the control eyes. urthermore, no significant differences ($p\leq0.05$) in the radiotracer accumulation were found between the non-ligated eyes of the control and surgical groups. In contrast, 10 days after the surgery, increased ^{68}Ga-NOTA-c(NGR) uptake (SUVmean=0.23±0.06) was found in the non-ligated eyes (non-I/R) of the surgical group (Figure 1B). The SUVmean values of the left (SUVmean=0.11±0.05) and right (SUVmean=0.09±0.02) eyes of the non-surgical control group remained approximately two-times lower compared to that of the eyeballs in the surgical group.

In vivo assessment of $\alpha_V\beta_3$ integrin receptor expression in the surgically induced rat model using ^{68}Ga-NODAGA-[c(RGD)]$_2$. For the determination of the expression of the neo-angiogenic marker $\alpha_V\beta_3$ integrin receptor, *in vivo* ^{68}Ga-

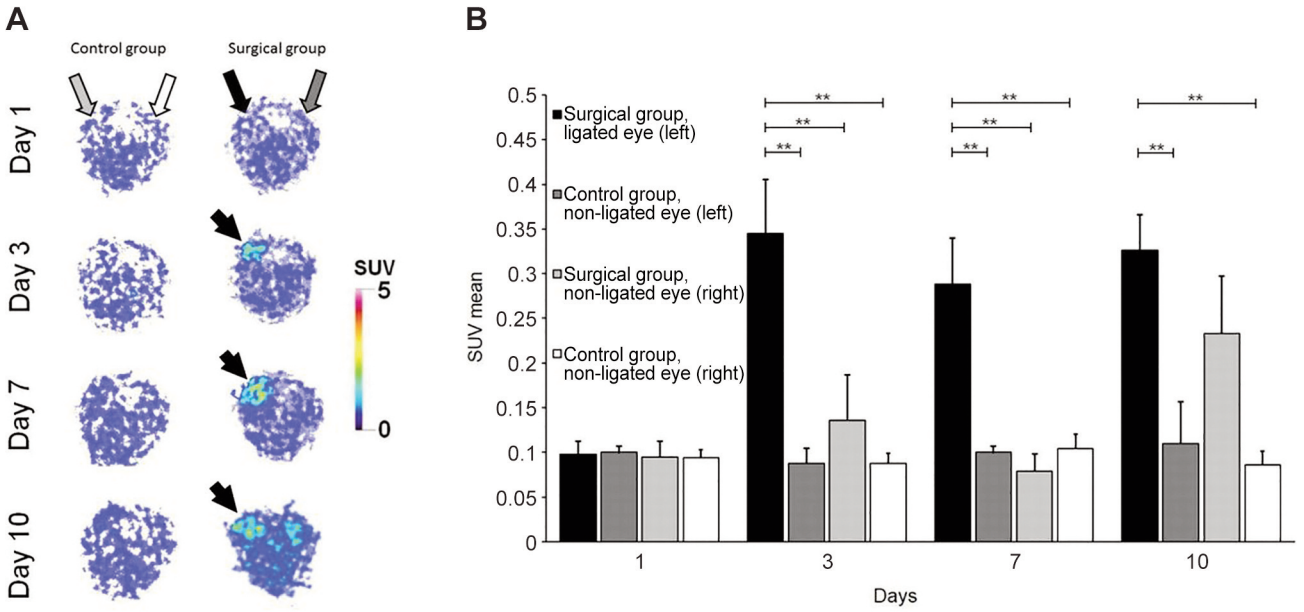

Figure 1. *PET imaging following NGR administration. (A) Representative transaxial decay-corrected PET images of the control (A panel, left) and surgical group (A panel, right) 1, 3, 7 and 10 days after ocular I/R surgery and 90 min after intravenous injection of ^{68}Ga-NOTA-c(NGR). Black arrow points to the ligated eye (I/R) of the surgical group, dark grey arrow points to the non-ligated eye (non-I/R) of the surgical group, grey arrow points to the non-ligated eye (non-I/R) of the (non-surgical)control group, white arrow points to the non-ligated eye (non-I/R) of the (non-surgical) control group. (B) Quantitative analysis of the PET images 1, 3, 7 and 10 days after ocular I/R surgery and 90 min after intravenous injection of ^{68}Ga-NOTA-c(NGR). PET: Position emmission tomography; SUV: standard uptake value; I/R: ischemia/reperfusion. Significance levels: p≤0.05 (*) and p≤0.01 (**).*

NODAGA-[c(RGD)]$_2$-PET imaging was used. The qualitative analysis of the decay-corrected PET images showed no significant accumulation in the ligated eyes of the surgical group 10 days after the surgically-induced I/R (Figure 2A). This observation was confirmed by the quantitative SUV analysis, where no significant differences (at p≤0.05) were found in the SUVmean values neither between the ligated (SUVmean=0.61±0.08) and non-ligated (SUVmean=0.57±0.07) eyes of the surgical group, nor between the surgical and non-surgical control groups (SUVmean=0.60±0.08) (Figure 2B).

Signal-to-background ratio analysis. Decay-corrected PET images were also evaluated for signal-to-background ratio (SBR). In case of the APN/CD13 specific ^{68}Ga-NOTA-c(NGR) molecule, we found that the SBR ratio in the surgical group was significantly higher (p≤0.05) on the 3rd (SBR=2.65±0.65) and 7th (SBR=3.51±0.99) days after the surgery compared to the SBR values of the non-surgical control group at the same investigated time points. Ten days after the surgery also high SBR value (SBR=2.11±0.95) was also observed in the surgical group, but this difference was not significant when it was compared to the non-surgical control group. The SBR values of the non-operated control group remained unchanged, suggesting no specific ^{68}Ga-NOTA-c(NGR) accumulation (Figure 3A). By using the $\alpha_V\beta_3$ integrin receptor specific tracer, ^{68}Ga-NODAGA-[c(RGD)]$_2$, we found no significant differences (at p≤0.05) in the SBR values between the surgical and non-surgical control groups 10 days after ocular I/R (Figure 3B).

Western blot and histopathological analysis of APN/CD13 expression. The expression of the neo-angiogenic molecules was analyzed by western blot 10 days after the surgery. Western blot analysis of APN/CD13 expression in ocular tissue revealed a significantly higher amount of APN/CD13 protein in the ligated bulbi of the surgically induced group than in the non-ligated bulbi (p<0.05) of the same animals as well as control groups (Figure 4A and B). No difference was observed between the non-ligated eyes of the surgically induced group and the control group. Histological examination showed severe retinal damage in the ganglion cell layer, inner plexiform layer, and in the nuclear layers (Figure 4C). In contrast, analysis of integrin expression in the experimental groups, demonstrated no difference in the α_V and β_3 integrin receptor expression between the surgical and control groups (Figure 4D and F).

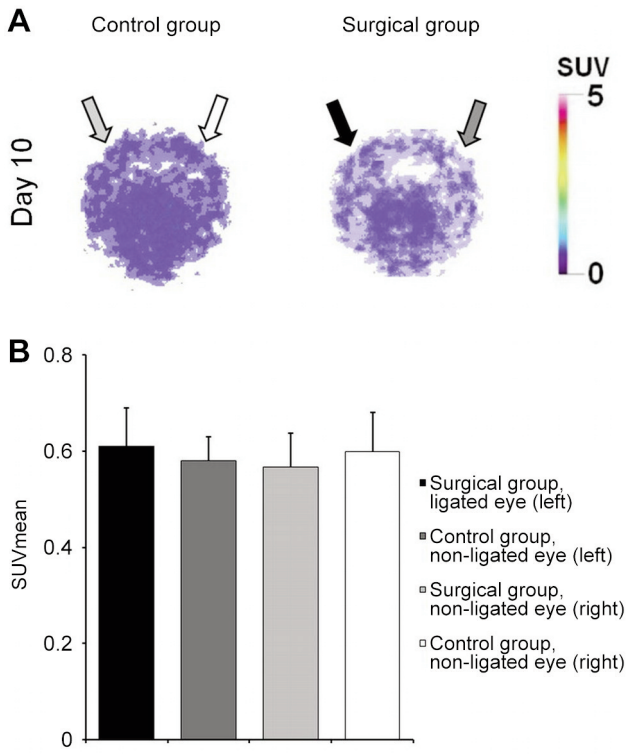

Figure 2. *PET imaging following RGD administration. (A) Representative transaxial decay-corrected PET images of the control (A panel, left) and surgical group (A panel, right) 10 days after ocular I/R surgery and 90 min after the intravenous injection of ^{68}Ga-NODAGA-[c(RGD)]$_2$. Black arrow points to the ligated eye (I/R) of the surgical group, dark grey arrow points to the non-ligated eye (non-I/R) of the surgical group, grey arrow points to the non-ligated eye (non-I/R) of the (non-surgical) control group, white arrow points to non-ligated eye (non-I/R) of the (non-surgical) control group. (B) Quantitative analysis of the PET images 10 days after ocular I/R surgery and 90 min after intravenous injection of ^{68}Ga-NODAGA-[c(RGD)]$_2$. PET: Position emmission tomography; SUV: standard uptake value; I/R: ischemia/reperfusion.*

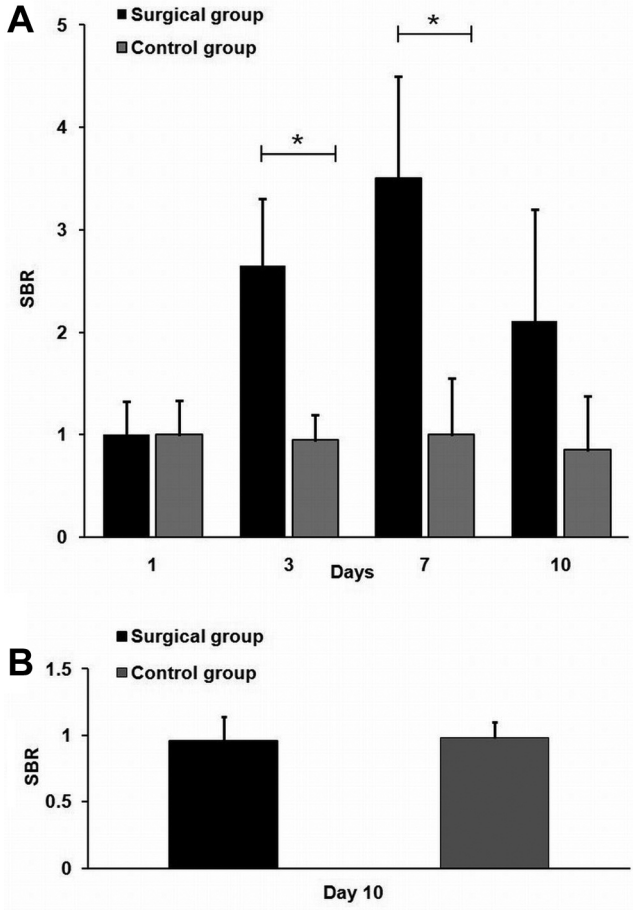

Figure 3. *Quantitative assessment of SBR. Assessment 1, 3, 7 and 10 days after ocular I/R using ^{68}Ga-NOTA-c(NGR) (A), and 10 days after ocular I/R using ^{68}Ga-NODAGA-[c(RGD)]$_2$ (B) PET imaging. SBR: Signal-to-background ratio; SUV: standard uptake value; I/R: ischemia/reperfusion. Significance level: p≤0.05 (*).*

Discussion

Diabetic retinopathy is a microvascular complication of diabetes mellitus and plays a crucial role in patients' diabetes-related vision loss. Abnormal vascular growth, angiogenesis, and the presence of hypoxia in the retina are strongly associated with the development of DR (7, 35). It has been previously reported that in diabetes high blood glucose level induces hypoxia, resulting in elevated expression of pro-angiogenic factors, such as vascular endothelial growth factor (VEGF), angiopoietin-2 (Ang-2), platelet-derived growth factor (PDGF), and others, in retinal tissues and vitreous bodies (35, 36). Moreover, previous studies have shown that due to the NGR peptide specific binding to APN and the RGD peptide to $\alpha_V\beta_3$ integrin, radiolabeled forms of these peptides are suitable for the *in vivo* detection of the neo-angiogenic processes in ischemia models. Based on these observations, the aim of this work was to determine *in vivo* the expression level of hypoxia-induced angiogenic factor APN/CD13 in the ischemia-reperfusion rat model with ^{68}Ga-NOTA-c(NGR) (14, 18) using PET imaging. This present study demonstrates a proof of concept for the use of ^{68}Ga-labeled cyclic NGR peptide – as a specific ligand of the APN/CD13 – for noninvasive PET imaging of diabetic retinopathy.

For the evaluation of the temporal changes in the expression of APN/CD13 in the surgically induced rat model *in vivo* PET imaging was used. In the field of *in vivo* ischemia-associated angiogenesis research, well-characterized rodent retina models have been used extensively to study both the physiological and pathological processes of angiogenesis. One of the most commonly used models is the ligation of the

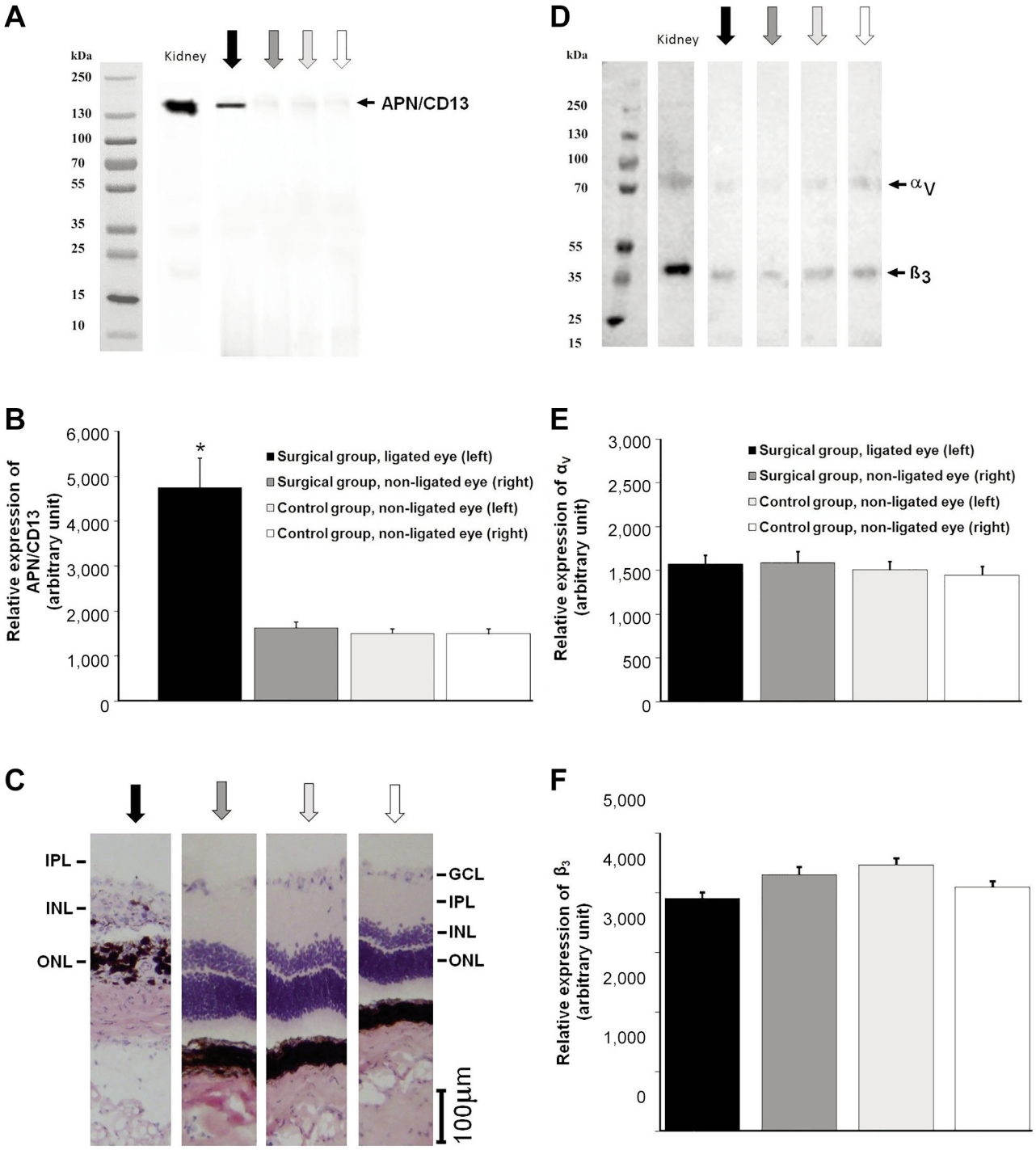

Figure 4. *Western blot and histopathological analysis of neo-angiogenic marker expression of the ligated and non-ligated eyes of the experimental groups 10 days after the surgery. (A) APN/CD13 expression. (B) Schematic diagram of arbitrary unit values of APN/CD13 expression (quantitative western blot analysis). (C) Representative hematoxylin-eosin staining of the ligated and non-ligated eyes of the experimental groups, showing severe retinal damage in the ganglion cell layer, inner plexiform layer, and in the nuclear layers. (D) Alpha$_V\beta_3$ integrin receptor expression. (E) and (F) Schematic diagram of arbitrary unit values of α_V and β_3 integrin receptor expression, respectively (quantitative western blot analysis). Black arrow: ligated eye (I/R) of the surgical group, dark grey arrow: non-ligated eye (non-I/R) of the surgical group, grey arrow: non-ligated eye (non-I/R) of the (non-surgical) control group, white arrow: non-ligated eye (non-I/R) of the (non-surgical) control group. I/R: Ischemia/reperfusion. Significance level: p≤0.05 (*). GCL: Ganglion cell layer; IPL: inner plexiform layer; INL: inner nuclear layer; ONL: outer nuclear layer.*

blood vessel that accompanies the optic nerve in retina (37, 38). In this longitudinal study the ligated eye model was used. The investigated time-points (days: 1, 3, 7 and 10 after I/R) were chosen due to the APN/CD13 expression peak expected within the first week and decreasing thereafter in other types of ischemic models, such as in the hindlimb (21) and myocardium (18). PET visual evaluation confirmed the presence of higher SUVmean values in the ocular region of the surgical group compared to control eyes. The left bulbus [ligated eye (I/R)] was adequately visualized using ^{68}Ga-NOTA-c(NGR), indicating a preferential binding of the tracer within the injured retina. In the same experimental animals, the non-ligated eyes (non-I/R) showed the same SUVmean values as the background values. In the non-surgical group, non-ligated bulbi gave similar results to the non-ligated eyes from the surgical group.

In the longitudinal study, both the surgically induced and the control groups were examined. Internal standard was used for further comparison. On the first day, no significant differences were observed between the groups used in the present study. Based on the given data the baseline values of the longitudinal study has been successfully developed. On the other time-points the results corresponded to the hypothesis; statistically significant differences ($p<0.05$) were found between ligated (I/R) and non-ligated bulbi (non-I/R) of the surgical group, moreover, no significant differences were acquired between the non-ligated bulbi (non-I/R) of the surgical group and non-ligated bulbi (non-I/R) of the control group. Interestingly, 10 days after the surgery increased ^{68}Ga-NOTA-c(NGR) uptake was found in the non-ligated eyes (non-I/R) of the surgical group. Possible cellular (*e.g.*, changes in the blood flow of the optic nerve head and preganglionic neurons) and physiological autoregulation mechanisms (*e.g.*, depolarization of vascular smooth muscle cells initiated by myogenic constriction, and choroidal response) may affect the results (39-41). Furthermore, APN/CD13 has been shown to be involved in the degradation of the extracellular matrix, which affects the permeability of the blood-retinal barrier (42, 43).

SBR values demonstrate how the quality of PET images can be evaluated, as the lower background accumulation makes it easier to evaluate them. Our data demonstrated that, the SBR value reached the maximum on the 7th day following ligation. This was expected, since other studies have shown the same angiogenic potential, investigated in rats with forelimb ischemia using ^{68}Ga-NOTA-c(RGDyK), and high $\alpha_V\beta_3$ expression was detected by immunohistochemical analysis 7 days after the surgery (44). The SBR values of the unoperated control group remained unchanged, suggesting no specific ^{68}Ga-NOTA-c(NGR) accumulation.

The specific binding of ^{68}Ga-NODAGA-[c(RGD)]$_2$ to $\alpha_V\beta_3$ integrin receptor is already known (45), thus, the assessment of the radiotracer specificity was performed to exclude the possibility of non-specific binding *in vivo*. In the PET specificity assessment study for SUVmean and SBR, no significant differences were found between any of the experimental models in the surgical group (non-I/R & I/R eyes) and control group (non-I/R eyes). Due to the fact that no differences were found in the SBR values between the non-ligated eyes (both in the surgical and non-surgical groups) when using ^{68}Ga-NODAGA-[c(RGD)]$_2$ and ^{68}Ga-NOTA-c(NGR) tracers, we concluded that the non-specific binding of ^{68}Ga-NOTA-c(NGR) in our experimental model could be excluded. Although not all aspects of I/R-induced hypoxia-mediated angiogenesis are known, it is known that in I/R renal and cardiac injury models, angiogenic factors, such as VEGF, are activated in the early and late stages after I/R to stabilize the microcirculation and blood supply in the affected areas (46, 47).

Western blot analysis of APN/CD13 expression in ocular tissue revealed more significant amounts of APN/CD13 protein in the ligated compared to the non-ligated bulbi, which correlated with the PET uptake values. Differences in APN/CD13 expression between the non-ligated eyes of the surgical and control groups were not observed. The western blot was performed to determine the presence of the integrin receptor expression. Equally low protein concentration was measured in all groups that was significantly lower compared to the amount of the kidney sample, used as positive control. Based on our results, it could be concluded that ^{68}Ga-NODAGA-[c(RGD)]$_2$ can be applicable as a negative control since no accumulation was observed in the PET images. while, western blot analysis did not reveal any $\alpha_V\beta_3$ integrin expression, which is the target of the ^{68}Ga-NODAGA-[c(RGD)]$_2$ radiopharmaceutical. Histological findings confirmed the ischemia-induced injury of the ligated eyes in the operated group. Similar histological results have been described in the literature, where, after ischemia, the thickness of the retina and the density of cells in different layers of the retina significantly decreased even after 60 min of ligation (48).

Based on our current knowledge, this is the first research to use an NGR sequence-containing peptide for PET imaging of I/R mediated APN/CD13 receptor expression in a surgically-induced retinopathy model. Currently, the identification and verification of angiogenic processes with *in vivo* imaging have high relevance (49). Our study shows that ^{68}Ga-labeled NGR motif is a useful radiotracer for the molecular imaging of APN/CD13 expression in retinopathy. The demonstration of the increased SUV values in the injured retina of the experimental animals could support the fact that APN/CD13 has a role in the pathogenic development of diabetic retinopathy in humans as well. Further studies are, of course, required to assess the prognostic utility of changes in NGR uptake after I/R and the development of DR in patients.

In conclusion, this is the first report to demonstrate the feasibility of PET with ^{68}Ga-NOTA-c(NGR) regarding noninvasive and sequential determination of APN/CD13 expression in a surgically-induced animal model of diabetic retinopathy. This technique will help better understand the I/R-mediated receptor expression and the function of APN/CD13 in diabetic retinopathy. This may provide an opportunity for an early stage diagnosis before the appearance of anatomical lesions.

Conflicts of Interest

The Authors declare no conflicts of interest.

Authors' Contributions

GF: Visualization, Investigation, Conceptualization, Writing - Original Draft; ND, SzR, AK, JPSz, GO, GV: Methodology, Visualization, Investigation; LB: Validation; IK and GM: Writing- Reviewing and Editing; JH and GyT: Writing- Reviewing and Editing.

Acknowledgements

The published work was supported by the EFOP-3.6.3-VEKOP-16-2017-00009 fund of European Union, by the NKFIH K119552 grant of the European Social Fund and National Research, Development and Innovation Office, and by the Thematic Excellence Programme (TKP2020-NKA-04) of the Ministry for Innovation and Technology in Hungary.

References

1 Blair M: Diabetes mellitus review. Urol Nurs *36(1)*: 27-36, 2016. PMID: 27093761.

2 DeFronzo RA, Ferrannini E, Groop L, Henry RR, Herman WH, Holst JJ, Hu FB, Kahn CR, Raz I, Shulman GI, Simonson DC, Testa MA and Weiss R: Type 2 diabetes mellitus. Nat Rev Dis Primers *1*: 15019, 2015. PMID: 27189025. DOI: 10.1038/nrdp.2015.19

3 Kitabchi AE, Umpierrez GE, Miles JM and Fisher JN: Hyperglycemic crises in adult patients with diabetes. Diabetes Care *32(7)*: 1335-1343, 2009. PMID: 19564476. DOI: 10.2337/dc09-9032

4 Ribeiro L, Bandello F, Tejerina AN, Vujosevic S, Varano M, Egan C, Sivaprasad S, Menon G, Massin P, Verbraak FD, Lund-Andersen H, Martinez JP, Jürgens I, Smets E, Coriat C, Wiedemann P, Ágoas V, Querques G, Holz FG, Nunes S, Neves C, Cunha-Vaz J and Evicr Net Study Group: Characterization of retinal disease progression in a 1-year longitudinal study of eyes with mild nonproliferative retinopathy in diabetes type 2. Invest Ophthalmol Vis Sci *56(9)*: 5698-5705, 2015. PMID: 26322834. DOI: 10.1167/iovs.15-16708

5 IDF Diabetes Atlas Group: Update of mortality attributable to diabetes for the IDF Diabetes Atlas: Estimates for the year 2013. Diabetes Res Clin Pract *109(3)*: 461-465, 2015. PMID: 26119773. DOI: 10.1016/j.diabres.2015.05.037

6 Saaddine JB, Honeycutt AA, Narayan KM, Zhang X, Klein R and Boyle JP: Projection of diabetic retinopathy and other major eye diseases among people with diabetes mellitus: United States, 2005-2050. Arch Ophthalmol *126(12)*: 1740-1747, 2008. PMID: 19064858. DOI: 10.1001/archopht.126.12.1740

7 Cheung N, Mitchell P and Wong TY: Diabetic retinopathy. Lancet *376(9735)*: 124-136, 2010. PMID: 20580421. DOI: 10.1016/S0140-6736(09)62124-3

8 Wong TY, Mwamburi M, Klein R, Larsen M, Flynn H, Hernandez-Medina M, Ranganathan G, Wirostko B, Pleil A and Mitchell P: Rates of progression in diabetic retinopathy during different time periods: a systematic review and meta-analysis. Diabetes Care *32(12)*: 2307-2313, 2009. PMID: 19940227. DOI: 10.2337/dc09-0615

9 Corti A, Pastorino F, Curnis F, Arap W, Ponzoni M and Pasqualini R: Targeted drug delivery and penetration into solid tumors. Med Res Rev *32(5)*: 1078-1091, 2012. PMID: 21287572. DOI: 10.1002/med.20238

10 Pasqualini R, Koivunen E, Kain R, Lahdenranta J, Sakamoto M, Stryhn A, Ashmun RA, Shapiro LH, Arap W and Ruoslahti E: Aminopeptidase N is a receptor for tumor-homing peptides and a target for inhibiting angiogenesis. Cancer Res *60(3)*: 722-727, 2000. PMID: 10676659.

11 Kapp TG, Rechenmacher F, Neubauer S, Maltsev OV, Cavalcanti-Adam EA, Zarka R, Reuning U, Notni J, Wester HJ, Mas-Moruno C, Spatz J, Geiger B and Kessler H: A comprehensive evaluation of the activity and selectivity profile of ligands for RGD-binding integrins. Sci Rep *7*: 39805, 2017. PMID: 28074920. DOI: 10.1038/srep39805

12 Arap W, Pasqualini R and Ruoslahti E: Cancer treatment by targeted drug delivery to tumor vasculature in a mouse model. Science *279(5349)*: 377-380, 1998. PMID: 9430587. DOI: 10.1126/science.279.5349.377

13 Metaferia BB, Rittler M, Gheeya JS, Lee A, Hempel H, Plaza A, Stetler-Stevenson WG, Bewley CA and Khan J: Synthesis of novel cyclic NGR/RGD peptide analogs *via* on resin click chemistry. Bioorg Med Chem Lett *20(24)*: 7337-7340, 2010. PMID: 21050757. DOI: 10.1016/j.bmcl.2010.10.064

14 Máté G, Kertész I, Enyedi KN, Mező G, Angyal J, Vasas N, Kis A, Szabó É, Emri M, Bíró T, Galuska L and Trencsényi G: *In vivo* imaging of Aminopeptidase N (CD13) receptors in experimental renal tumors using the novel radiotracer (68)Ga-NOTA-c(NGR). Eur J Pharm Sci *69*: 61-71, 2015. PMID: 25592229. DOI: 10.1016/j.ejps.2015.01.002

15 Ellis LM, Liu W, Ahmad SA, Fan F, Jung YD, Shaheen RM and Reinmuth N: Overview of angiogenesis: Biologic implications for antiangiogenic therapy. Semin Oncol *28(5 Suppl 16)*: 94-104, 2001. PMID: 11706401. DOI: 10.1016/s0093-7754(01)90287-8

16 Phelps ME: Positron emission tomography provides molecular imaging of biological processes. Proc Natl Acad Sci U.S.A. *97(16)*: 9226-9233, 2000. PMID: 10922074. DOI: 10.1073/pnas.97.16.9226

17 Owen DR and Matthews PM: Imaging brain microglial activation using positron emission tomography and translocator protein-specific radioligands. Int Rev Neurobiol *101*: 19-39, 2011. PMID: 22050847. DOI: 10.1016/B978-0-12-387718-5.00002-X

18 Grönman M, Tarkia M, Kiviniemi T, Halonen P, Kuivanen A, Savunen T, Tolvanen T, Teuho J, Käkelä M, Metsälä O, Pietilä M, Saukko P, Ylä-Herttuala S, Knuuti J, Roivainen A and Saraste A: Imaging of $\alpha_V\beta_3$ integrin expression in experimental myocardial ischemia with [^{68}Ga]NODAGA-RGD positron

emission tomography. J Transl Med *15(1)*: 144, 2017. PMID: 28629432. DOI: 10.1186/s12967-017-1245-1

19 Haubner R: Alphavbeta3-integrin imaging: a new approach to characterise angiogenesis? Eur J Nucl Med Mol Imaging *33 Suppl 1*: 54-63, 2006. PMID: 16791598. DOI: 10.1007/s00259-006-0136-0

20 Choe YS and Lee KH: Targeted *in vivo* imaging of angiogenesis: present status and perspectives. Curr Pharm Des *13(1)*: 17-31, 2007. PMID: 17266586. DOI: 10.2174/138161207779313812

21 Orbay H, Hong H, Zhang Y and Cai W: PET/SPECT imaging of hindlimb ischemia: focusing on angiogenesis and blood flow. Angiogenesis *16(2)*: 279-287, 2013. PMID: 23117521. DOI: 10.1007/s10456-012-9319-4

22 Association for Research in Vision and Ophthalmology ARVO: Statement for the Use of Animals in Ophthalmic and Visual Research, 2016. Available at: https://www.arvo.org/About/policies/statement-for-the-use-of-animals-in-ophthalmic-and-vision-research/ [Last accessed on December 22, 2021]

23 Varga B, Gesztelyi R, Bombicz M, Haines D, Szabo AM, Kemeny-Beke A, Antal M, Vecsernyes M, Juhasz B and Tosaki A: Protective effect of alpha-melanocyte-stimulating hormone (α-MSH) on the recovery of ischemia/reperfusion (I/R)-induced retinal damage in a rat model. J Mol Neurosci *50(3)*: 558-570, 2013. PMID: 23504281. DOI: 10.1007/s12031-013-9998-3

24 Kohen MC, Tatlipinar S, Cumbul A and Uslu Ü: The effects of bevacizumab treatment in a rat model of retinal ischemia and perfusion injury. Mol Vis *24*: 239-250, 2018. PMID: 29681725.

25 Lin LT, Chen JT, Tai MC, Chen YH, Chen CL, Pao SI, Hsu CR and Liang CM: Protective effects of hypercapnic acidosis on Ischemia-reperfusion-induced retinal injury. PLoS One *14(1)*: e0211185, 2019. PMID: 30682118. DOI: 10.1371/journal.pone.0211185

26 Varga B, Priksz D, Lampé N, Bombicz M, Kurucz A, Szabó AM, Pósa A, Szabó R, Kemény-Beke Á, Remenyik J, Gesztelyi R and Juhász B: Protective effect of prunus cerasus (sour cherry) seed extract on the recovery of ischemia/reperfusion-induced retinal damage in zucker diabetic fatty rat. Molecules *22(10)*: 1782, 2017. PMID: 29065463. DOI: 10.3390/molecules22101782

27 Inokuchi Y, Shimazawa M, Nakajima Y, Komuro I, Matsuda T, Baba A, Araie M, Kita S, Iwamoto T and Hara H: A Na+/Ca2+ exchanger isoform, NCX1, is involved in retinal cell death after N-methyl-D-aspartate injection and ischemia-reperfusion. J Neurosci Res *87(4)*: 906-917, 2009. PMID: 18855935. DOI: 10.1002/jnr.21906

28 Ogishima H, Nakamura S, Nakanishi T, Imai S, Kakino M, Ishizuka F, Tsuruma K, Shimazawa M and Hara H: Ligation of the pterygopalatine and external carotid arteries induces ischemic damage in the murine retina. Invest Ophthalmol Vis Sci *52(13)*: 9710-9720, 2011. PMID: 22110078. DOI: 10.1167/iovs.11-8160

29 Zhang H, Sonoda KH, Qiao H, Oshima T, Hisatomi T and Ishibashi T: Development of a new mouse model of branch retinal vein occlusion and retinal neovascularization. Jpn J Ophthalmol *51(4)*: 251-257, 2007. PMID: 17660984. DOI: 10.1007/s10384-007-0445-2

30 Kumar P, Kumar S, Udupa E, Kumar U, Rao P and Honnegowda T: Role of angiogenesis and angiogenic factors in acute and chronic wound healing. Plastic and Aesthetic Research *2(5)*: 243, 2019. DOI: 10.4103/2347-9264.165438

31 Li J, Zhang YP and Kirsner RS: Angiogenesis in wound repair: angiogenic growth factors and the extracellular matrix. Microsc Res Tech *60(1)*: 107-114, 2003. PMID: 12500267. DOI: 10.1002/jemt.10249

32 Lajtos I, Czernin J, Dahlbom M, Daver F, Emri M, Farshchi-Heydari S, Forgacs A, Hoh CK, Joszai I, Krizsan AK, Lantos J, Major P, Molnar J, Opposits G, Tron L, Vera DR and Balkay L: Cold wall effect eliminating method to determine the contrast recovery coefficient for small animal PET scanners using the NEMA NU-4 image quality phantom. Phys Med Biol *59(11)*: 2727-2746, 2014. PMID: 24800813. DOI: 10.1088/0031-9155/59/11/2727

33 Gassmann M, Grenacher B, Rohde B and Vogel J: Quantifying Western blots: pitfalls of densitometry. Electrophoresis *30(11)*: 1845-1855, 2009. PMID: 19517440. DOI: 10.1002/elps.200800720

34 Wang R, Wu J, Chen Z, Xia F, Sun Q and Liu L: Postconditioning with inhaled hydrogen promotes survival of retinal ganglion cells in a rat model of retinal ischemia/reperfusion injury. Brain Res *1632*: 82-90, 2016. PMID: 26705611. DOI: 10.1016/j.brainres.2015.12.015

35 Abcouwer SF: Angiogenic factors and cytokines in diabetic retinopathy. J Clin Cell Immunol *Suppl 1(11)*: 1-12, 2013. PMID: 24319628. DOI: 10.4172/2155-9899

36 Crawford TN, Alfaro DV 3rd, Kerrison JB and Jablon EP: Diabetic retinopathy and angiogenesis. Curr Diabetes Rev *5(1)*: 8-13, 2009. PMID: 19199892. DOI: 10.2174/157339909787314149

37 Stahl A, Connor KM, Sapieha P, Chen J, Dennison RJ, Krah NM, Seaward MR, Willett KL, Aderman CM, Guerin KI, Hua J, Löfqvist C, Hellström A and Smith LE: The mouse retina as an angiogenesis model. Invest Ophthalmol Vis Sci *51(6)*: 2813-2826, 2010. PMID: 20484600. DOI: 10.1167/iovs.10-5176

38 Masuzawa K, Jesmin S, Maeda S, Kaji Y, Oshika T, Zaedi S, Shimojo N, Yaji N, Miyauchi T and Goto K: A model of retinal ischemia-reperfusion injury in rats by subconjunctival injection of endothelin-1. Exp Biol Med (Maywood) *231(6)*: 1085-1089, 2006. PMID: 16741054.

39 Kur J, Newman EA and Chan-Ling T: Cellular and physiological mechanisms underlying blood flow regulation in the retina and choroid in health and disease. Prog Retin Eye Res *31(5)*: 377-406, 2012. PMID: 22580107. DOI: 10.1016/j.preteyeres.2012.04.004

40 Kergoat H: Electroretinogram in unilateral vascular stress in nondiabetic and diabetic subjects. Optom Vis Sci *70(9)*: 743-749, 1993. PMID: 8233370. DOI: 10.1097/00006324-199309000-00011

41 Lovasik JV, Kergoat H and Gagnon M: Experimentally reduced perfusion of one eye impairs retinal function in both eyes. Optom Vis Sci *82(9)*: 850-857, 2005. PMID: 16189496. DOI: 10.1097/01.opx.0000177810.58122.57

42 Trindade F, Ferreira R, Amado F and Vitorino R: Biofluid proteases profiling in diabetes mellitus. Adv Clin Chem *69*: 161-207, 2015. PMID: 25934362. DOI: 10.1016/bs.acc.2014.12.004

43 Hossain A, Heron D, Davenport I, Huckaba T, Graves R, Mandal T, Muniruzzaman S, Wang S and Bhattacharjee PS: Protective effects of bestatin in the retina of streptozotocin-induced diabetic mice. Exp Eye Res *149*: 100-106, 2016. PMID: 27344955. DOI: 10.1016/j.exer.2016.06.016

44 Kim JH, Kim YH, Kim YJ, Yang BY, Jeong JM, Youn H, Lee DS and Lee JS: Quantitative positron emission tomography

imaging of angiogenesis in rats with forelimb ischemia using (68)Ga-NOTA-c(RGDyK). Angiogenesis *16(4)*: 837-846, 2013. PMID: 23857293. DOI: 10.1007/s10456-013-9359-4

45 Velikyan I and Lindhe Ö: Preparation and evaluation of a ^{68}Ga-labeled RGD-containing octapeptide for noninvasive imaging of angiogenesis: biodistribution in non-human primate. Am J Nucl Med Mol Imaging *8(1)*: 15-31, 2018. PMID: 29531858.

46 Pallet N, Thervet E and Timsit MO: Angiogenic response following renal ischemia reperfusion injury: new players. Prog Urol *24 Suppl 1*: S20-S25, 2014. PMID: 24950928. DOI: 10.1016/S1166-7087(14)70059-4

47 Kobayashi K, Maeda K, Takefuji M, Kikuchi R, Morishita Y, Hirashima M and Murohara T: Dynamics of angiogenesis in ischemic areas of the infarcted heart. Sci Rep *7(1)*: 7156, 2017. PMID: 28769049. DOI: 10.1038/s41598-017-07524-x

48 Hughes WF: Quantitation of ischemic damage in the rat retina. Exp Eye Res *53(5)*: 573-582, 1991. PMID: 1743256. DOI: 10.1016/0014-4835(91)90215-z

49 Hu TT, Vanhove M, Porcu M, Van Hove I, Van Bergen T, Jonckx B, Barbeaux P, Vermassen E and Feyen JHM: The potent small molecule integrin antagonist THR-687 is a promising next-generation therapy for retinal vascular disorders. Exp Eye Res *180*: 43-52, 2019. PMID: 30472075. DOI: 10.1016/j.exer.2018.11.022

Received October 29, 2021
Revised December 6, 2021
Accepted December 22, 2021